

Evaluation of the Hartree–Fock Dispersion (HFD) Model as a Practical Tool for Probing Intermolecular Potentials of Small Aromatic Clusters: Comparison of the HFD and MP2 Intermolecular Potentials

Carlos Gonzalez

Physical and Chemical Properties Division, National Institute of Standards and Technology,
Gaithersburg, Maryland 20899

Edward C. Lim*,†

Department of Chemistry and The Center for Laser and Optical Spectroscopy, The University of Akron,
Akron, Ohio 44325-3601

Received: May 8, 2003; In Final Form: August 21, 2003

The performance of the Hartree–Fock dispersion (HFD) model for aromatic clusters has been evaluated by comparing the HFD/6-31G intermolecular potentials with the MP2/6-31G potentials for dimers of four aromatic hydrocarbons (benzene, naphthalene, anthracene, and pyrene) and the trimer of naphthalene. The computationally efficient HFD model yields equilibrium geometries and binding energies that are essentially identical to those from the MP2 calculations for all aromatic clusters. For the T-shaped dimer of benzene and the cyclic trimer of naphthalene for which experimental geometries are known, the computed geometry and intermolecular separations are in excellent agreement with the experimental data. Although the MP2/6-31G (not corrected for basis set superposition errors) and HFD/6-31G binding energies (D_e) of the dimers of benzene and naphthalene, and the trimer of naphthalene, are almost a factor of 2 greater than the experimental values (D_0), they are considerably in better agreement with experiment than the MP2 interaction energies computed by using larger and diffuse basis sets, 6-31G* (0.25) and aug-cc-pVDZ. The calculated minimum-energy structures of the four aromatic hydrocarbons of differing sizes support the notion that electrostatic interaction favors edge-on (T-shaped) structures, whereas dispersion interaction favors stacked structures. The computed dimer binding energy is approximately a linear function of the number of hexagons in the monomer.

1. Introduction

Aromatic–aromatic interactions play an important role in many chemical and biological systems. They control, among others, structures of DNA and proteins, the packing of aromatic crystals, the formation of aggregates, the binding affinities in host–guest systems, and conformational preferences of poly-aromatic macrocycles and chain molecules.

As the species formed by a direct consequence of the intermolecular interactions, the geometrical structures and binding energies of aromatic clusters provide fundamental understanding of aromatic π – π interactions. For this reason aromatic dimers and higher clusters, produced by supersonic jet expansion, have been the focus of substantial experimental and computational efforts. Experimental information on the interaction potentials is however sparse, being limited only to the T-shaped dimer of benzene¹ and the cyclic trimer of naphthalene,² Figure 1.

Computationally, the most accurate methods for determining the geometry and binding energy of aromatic dimers and higher clusters are correlated quantum chemistry calculations that use very large correlation-consistent basis sets. Correlated calculations are essential to account for the dispersion interaction that



Figure 1. Equilibrium geometries of the T-shaped (C_{2v}) benzene dimer and cyclic (C_{3h}) trimer of naphthalene, as deduced from the microwave spectroscopy¹ and rotational coherence spectroscopy,² respectively.

is the major source of attraction in van der Waals (vdW) molecules, whereas very large basis sets are necessary to minimize both the basis set convergence error and basis set superposition error (BSSE).³ Such high-level calculations are possible for benzene dimers, and there have been a large number of theoretical studies for these species.⁴ The most elaborate of these is the work of Sherrill and co-workers.⁵ Using explicitly correlated MP2-R12/A techniques, they investigated the basis set and electron correlation effects for the benzene dimer. The CCSD(T) binding energies (D_e) at the basis set limit have been deduced to be 11.46 and 11.63 kJ/mol for the T-shaped and parallel displaced (PD) configurations, respectively. These interaction energies are in excellent agreement with the experimental binding energy measured by Grover et al. ($D_0 \cong 10.0$ kJ/mol).⁶ In a closely related calculation using basis set

* To whom correspondence should be addressed. FAX: 330-972-6407.
E-mail: elim@uakron.edu.

† Holder of the Goodyear Chair in Chemistry at The University of Akron.

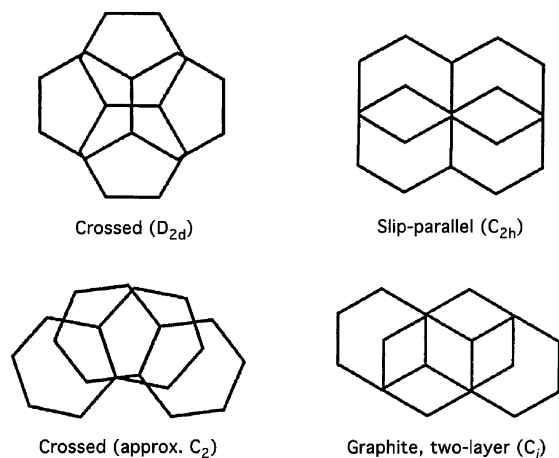


Figure 2. Fully optimized low-energy conformers of naphthalene, as obtained from the MP2/6-31G and HFD/6-31G calculations.

extrapolations and rigid monomer geometry optimizations, Tsuzuki et al.⁷ obtained CCSD(T) binding energies at the basis set limit that are slightly smaller (10.29 kJ/mol for T and 10.38 kJ/mol for PD).

Unfortunately, for the dimers and higher clusters of polycyclic aromatic hydrocarbons, similar correlated quantum chemistry calculations using large basis sets are not practical or possible. For these species, use of small basis sets is the only practical option available for correlated calculations that are necessary for describing vdW interactions. In the first ab initio study of the polycyclic vdW clusters, we have probed the fully optimized equilibrium geometries of naphthalene trimer at the MP2/6-31G level of theory.⁸ The global minimum, obtained without the BSSE correction, was found to be the cyclic structure with C_{3h} symmetry in which the long axes of the monomers are parallel. Interestingly, the predicted minimum-energy structure is essentially identical to the experimental geometry obtained from rotational coherence spectroscopy.² The computed and experimental rotation constants (B and C) differ only by about 0.4%.

Extension of the MP2/6-31G calculations to the dimers of naphthalene and anthracene yielded the D_{2d} crossed structure and C_{2h} slip-parallel (parallel-displaced) structure of similar energies,⁹ Figure 2. Recently, Kim and co-workers¹⁰ computed the MP2 interaction energy of the naphthalene dimer using two basis sets: 6-31G* and 6-31G* (0.25), which is the 6-31G* basis with exponent on the d function reduced to 0.25. The geometry optimization in their work was constrained to the rigid monomers translated along the three Cartesian axes. The global minimum, based on the counterpoise-corrected (CP-corrected) interaction energy, is a distorted graphite two-layer (GTL) structure of C_i symmetry, Figure 2, with the crossed dimer of C_s symmetry having slightly higher energy. More recently, using MP2/6-31G* geometries, Walsh¹¹ carried out CP-corrected single-point energy calculations at the MP2 level of theory with the 6-31G* (0.25) basis and with a larger basis consisting of aug-cc-pVDZ basis on carbons and cc-pVDZ basis on hydrogens. The two lowest energy structures so obtained are a distorted crossed geometry with approximate C_2 symmetry, which is the global minimum, and the C_i graphite two-layer structure, Figure 2. It is not known whether the discrepancies between the predicted structures from these studies is the result of (a) using a small basis set (Gonzalez and Lim), (b) not implementing full geometry optimization (Lee et al. and Walsh), (c) CP correction for BSSE (Lee et al. and Walsh), or (d) simply missing some candidate structures in the geometry search (Gonzalez and Lim).

Because of the size of the species, the ab initio calculations even at the modest MP2/6-31G level of theory are prohibitive for aromatic clusters larger than naphthalene trimer or anthracene dimer. For larger aromatic clusters, it is therefore essential to apply computationally efficient methods. A particularly promising practical method, which we have recently introduced to the structural search of aromatic clusters,¹² is the Hartree–Fock dispersion (HFD) model proposed originally by Hepburn et al.¹³ In this model, the interaction between the molecules in the cluster is described by the computationally efficient SCF (HF) calculation and the worst deficiency of SCF—i.e., the lack of treatment of electron correlation—is corrected by adding an empirical London dispersion term in a perturbative manner.¹⁴ The first application of the HFD/6-31G model to the qualitative structural probe of the dimers of benzene and naphthalene has been very promising.¹²

To better understand the effects of basis sets and BSSE corrections on MP2 intermolecular potentials and to assess the quantitative utility of the simple HFD model, we have recently computed the equilibrium geometries and binding energies of the van der Waals (vdW) dimers of benzene, naphthalene, anthracene, and pyrene, as well as those of the naphthalene trimer. This paper describes the results of these computations and their comparison to the available experimental data, which demonstrate the utility of the computationally efficient HFD model for probing intermolecular potentials of small aromatic clusters.

2. Computational Methods

Full geometry optimizations were carried out at the MP2/6-31G level of theory using redundant internal coordinates¹⁵ as implemented in the Gaussian 98 suite of quantum chemistry programs.^{16,17} The geometry optimizations at the HFD/6-31G level were carried out with a routine implemented into the quantum chemistry package GAMESS.¹⁸ In each case, the monomer geometries were optimized at the same level of theory. Details of the implementation of our HFD method are given elsewhere.¹² Briefly, to account for dispersion forces in the ab initio Hartree–Fock formalism, an energy term, U_{disp} , is added perturbatively at the end of the SCF procedure. For a molecular cluster, the total electronic energy E_{HFD} is therefore

$$E_{\text{HFD}} = E_{\text{HF}} + U_{\text{disp}} f_n \quad (1)$$

where E_{HF} is the Hartree–Fock energy, U_{disp} is the dispersion energy, and f_n is a damping function used to avoid singularities in the dispersion energy at small interatomic distances. The dispersion energy was obtained using the expression

$$U_{\text{disp}} = - \sum_{\mu=1}^{\text{NMOL}-1} \sum_{\nu=\mu+1}^{\text{NMOL}} \sum_{i=1}^{\text{NAT}_{\mu}} \sum_{j=1}^{\text{NAT}_{\nu}} \left\{ \sum_{n=6,8,10} \frac{[C_{ij}^n C_{ji}^n]^{1/2}}{R_{ij}^n} \right\} \quad (2)$$

Here NMOL is the number of molecules in the cluster, NAT_{μ} is the total number of atoms for molecule μ , R_{ij} is the distance between atoms i and j in molecules μ and ν respectively, and the coefficients are the n -order dispersion coefficients corresponding to atom i and j . In our work, the dispersion term in eq 2 is truncated to the lowest order ($n = 6$). For C–C, H–H, and C–H interactions, we have used the dispersion coefficients reported by Huiszoon and Mulder¹⁹ ($C_6(\text{C–C}) = 2.17 \text{ J nm}^6 \text{ mol}^{-1}$, $C_6(\text{H–H}) = 0.167 \text{ J nm}^6 \text{ mol}^{-1}$, and $C_6(\text{C–H}) = 0.603 \text{ J nm}^6 \text{ mol}^{-1}$). No fitting to experiment was performed on this potential. For the damping function, we have adopted the simple two-parameter sigmoid function:

TABLE 1: Comparison of the MP2/6-31G and HFD/6-31G Intermolecular Potentials with Experiment for the C_{3h} Trimer of Naphthalene and C_{2v} Dimer of Benzene

method	naphthalene trimer ^a		benzene dimer ^a	
	intermoiety distance ^b (Å)	binding energy ^c (kJ/mol)	intermoiety distance ^b (Å)	binding energy ^c (kJ/mol)
MP2/6-31G//MP2/6-31G	4.99	67.96	5.01	10.9
HFD/6-31G//HFD/6-31G	4.86	68.27	5.00	11.7
experiment	4.93 ^d	36.2 ^e	4.96 ^f	6.8, ^g 10.0 ^h

^a See Figure 1 for the structure. ^b c.m. to c.m. distance. ^c BSSE-uncorrected interaction energy. ^d Reference 2. ^e Reference 21. ^f Reference 1. ^g Reference 20. ^h Reference 6.

$$f_6(R_{ij}) = \frac{1}{(1 + e^{\alpha(R_0 - R_{ij})})} \quad (3)$$

where R_{ij} is the distance between atoms i and j and α and R_0 are empirical parameters (1.5 bohr⁻¹ and 6.0 bohr, respectively).

The HFD routines were implemented in a local version of the GAMESS package running on an IBM RS/6000 model 270, whereas the MP2 calculations were performed with the GAUSS-IAN 98 suite of programs on a Cray T-94 at the Ohio Supercomputer Center.

3. Results and Discussion

A. Comparison of the MP2/6-31G and HFD/6-31G Intermolecular Potentials with Experiment. Since the experimental information concerning the intermolecular potentials of aromatic clusters is available only for the T-shaped (C_{2v}) dimer of benzene and the cyclic (C_{3h}) trimer of naphthalene, it is desirable to evaluate the performance of the computational methods by computing the geometry and binding energy of these species. Table 1 compares the MP2/6-31G and HFD/6-31G intermolecular potentials with each other and with experiment. The intermoiety distances and the binding energies, calculated by MP2/6-31G and HFD/6-31G, are in excellent agreement with each other. Thus, the intermolecular distances differ by less than 0.07 Å, and the binding energies agree within 0.3 kJ/mol. We consider it significant that the two rather different methodologies yield essentially identical intermolecular potentials for two clusters of different sizes and shapes. Moreover, the computed intermolecular distances agree with experiment within the uncertainty of the measurements. Where the computed values differ significantly from experiment is in the interaction energy. More specifically, the computed binding energies are almost a factor of 2 greater than the experimental values that are determined from the measurements of the ionization and appearance potentials.^{6,20,21} The results indicate that whereas the MP2 calculation with a small basis set (6-31G) may be adequate for describing geometry, basis sets much larger than 6-31G are required for the proper treatment of the interaction energy. This is in line with the conclusion of Sherrill and co-workers⁵ that basis sets such as aug-cc-pVDZ are sufficient for geometry optimization at the MP2 level, but basis sets larger than aug-cc-pVTZ are important for accurate binding energies. From the work of Tsuzuki and others, it is known that the MP2 calculations overestimate the dimer binding energy for both benzene⁷ and naphthalene.²²

B. Effects of Basis Sets and Counterpoise Corrections on MP2 Intermolecular Potentials of Naphthalene Dimers. To probe the origin of the discrepancies between the MP2 minimum-energy dimer structures of naphthalene computed with different basis sets (see Introduction), we have calculated the equilibrium geometries and binding energies of naphthalene dimers using 6-31G and 6-31G* (0.25) basis sets, and with and without the CP correction.

TABLE 2: Comparison of the BSSE-Uncorrected MP2/6-31G* (0.25) and MP2/6-31G Binding Energies (kJ/mol) of Naphthalene Dimers with Experiment

conformer ^a	MP2/6-31G* (0.25)// MP2/6-31G* (0.25)	MP2/6-31G// MP2/6-31G	expt ^b
crossed (approx C_2)	78.01	25.36	12.1
graphite (C_i)	75.81	23.65	
crossed (D_{2d})	60.27	21.23	
slip-parallel (C_{2h})	58.55	20.97	
crossed (C_s)	57.29	21.87	

^a See Figure 2 for the structures. ^b Reference 21.

Table 2 presents the binding energies of the fully optimized low-energy conformers of naphthalene dimers (Figure 2), computed at the MP2/6-31G* (0.25), and MP2/6-31G levels of theory, without the BSSE correction. The results are interesting for several reasons. First, the two lowest energy dimer structures obtained from the two levels of theory are the C_2 crossed dimer and the C_i graphite two-layer structure of slightly higher energy, consistent with the results of Walsh¹¹ based on 6-31G*(0.25) and aug-cc-pVDZ basis sets. Apparently, the C_i and C_2 conformers were missed in our original MP2/6-31G calculations due to possible deficiencies in the MM3 force field used in the initial search of the candidate structures. Second, the fully optimized crossed dimer of D_{2d} symmetry is a stationary point at the MP2/6-31G* (0.25) level, and it is more stable than the crossed dimer of C_s symmetry reported by Lee et al.¹⁰ Third, although the MP2/6-31G and MP2/6-31G* (0.25) calculations, without counterpoise corrections, lead to similar structures and ordering of the relative binding energies, the use of the 6-31G* (0.25) basis set yields dimer binding energies that are about a factor of 5 too large as compared to the experimental binding energy (~12 kJ/mol).²¹ Although BSSE corrections greatly reduce the interaction energies (and increase the intermoiety distances), the CP-corrected binding energies are still too large by about a factor of 3.^{10,11} On the other hand, MP2/6-31G calculations yield binding energies that are significantly closer to the experimental value. In comparing the experimental and computed binding energies, it is important to recognize that whereas the experimental value refers to the energy measured from the zero-point level (D_0), the computed value represents the energy measured from the potential minimum (D_e). Hence, the computed binding energy needs to be reduced by the zero-point energy for comparison with the experimental value. Unfortunately, because of the lack of accurate information concerning the vibrational frequencies, the magnitude of the zero-point energy correction is very difficult to estimate, but it is expected to be small (a few kilojoules per mole)²³ relative to D_e and D_0 .

It is interesting that the MP2 calculation with a small basis set (6-31G) and without the BSSE corrections yields interaction energies that are superior to the binding energies obtained using the larger, and diffuse, basis sets. This is believed to be due to a fortuitous, but systematic, cancellation of errors arising from

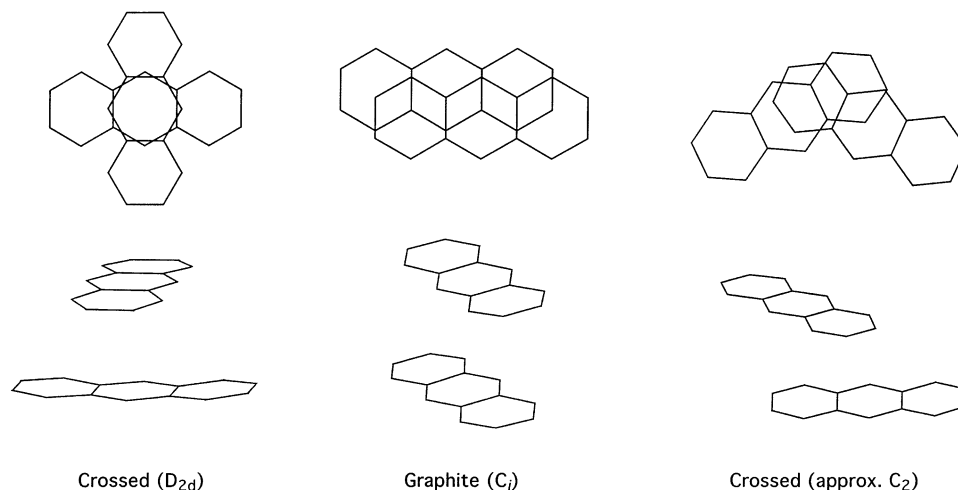


Figure 3. Top and side views of the low-energy M2/6-31G and HFD/6-31G dimer structures of anthracene.

TABLE 3: Comparison of the MP2/6-31G and HFD/6-31G Intermolecular Potentials for Naphthalene Dimers

conformer ^a	intermoeity distance ^b (Å)		binding energy ^c (kJ/mol)	
	MP2/6-31G	HFD/6-31G	MP2/6-31G	HFD/6-31G
crossed (approx C_2)	3.64	3.69	25.36	26.42
graphite (C_i)	3.83	3.90	23.65	25.65
crossed (D_{2d})	3.57	3.62	21.72	24.66
slip-parallel (C_{2h})	3.83	3.88	21.46	24.48

^a See Figure 2 for the structures. ^b c.m. to c.m. distance. ^c BSSE-uncorrected interaction energy.

a lack of convergence in the second-order perturbation theory and the deficiency in the basis set. In this connection, Dunning³ has recently conjectured that it is quite possible, and even probable, that binding energies computed without the CP correction are closer to the complete basis set limit than the corrected values, due to the fact that BSSE corrections and basis set convergence errors are often of opposite sign.

C. Comparison of the HFD/6-31G and MP2/6-31G Intermolecular Potentials. In view of the remarkable agreement between the HFD/6-31G and MP2/6-31G intermolecular potentials for the T-shaped benzene dimer and the cyclic naphthalene trimer, it is of interest to inquire whether the correspondence between MP2/6-31G and HFD/6-31G calculations extends to other aromatic clusters as well. To address this question, we have computed the equilibrium geometries and binding energies of the four low-energy dimer conformers of naphthalene and the three low-energy dimer conformers of anthracene and pyrene.

Table 3 compares the MP2/6-31G and HFD/6-31G intermolecular potentials of the four low-energy dimer conformers of naphthalene listed in Table 2. Remarkably, the relative conformer stability, the binding energy, and the center of mass intermolecular separation, obtained by the two methods, are essentially identical for all the dimer conformers. The intermoeity distances and the binding energies differ by less than 0.07 Å and 3 kJ/mol, respectively, for each conformer. It is fortunate that the computationally efficient HFD model yields intermolecular potentials that are so similar to those from the MP2 calculations.

Table 4 presents the results of the HFD/6-31G and MP2/6-31G geometry calculations for the anthracene dimers. The lowest energy conformer has the D_{2d} crossed structure,⁹ which is followed by the C_i parallel-displaced structure and the C_{2h}

TABLE 4: Comparison of the MP2/6-31G and HFD/6-31G Intermolecular Potentials for Anthracene Dimers

conformer ^a	intermoeity distance ^b (Å)		binding energy ^c (kJ/mol)	
	MP2/6-31G	HFD/6-31G	MP2/6-31G	HFD/6-31G
crossed (D_{2d})	3.30	3.32	42.24	44.57
graphite (C_i)	3.79	3.87	40.23	40.85
crossed (approx C_2)	4.52	4.50	34.57	35.24

^a See Figure 3 for the structures. ^b c.m. to c.m. distance. ^c BSSE-uncorrected interaction energy.

TABLE 5: Comparison of the MP2/6-31G and HFD/6-31G Intermolecular Potentials for Pyrene Dimers

conformer ^a	intermoeity distance ^b (Å)		binding energy ^c (kJ/mol)	
	MP2/6-31G	HFD/6-31G	MP2/6-31G	HFD/6-31G
slip-parallel, L (C_{2h})	3.79	3.86	54.84	51.00
graphite (C_i)	3.75	3.82	54.03	50.09
slip-parallel, S (C_{2h})	3.64	3.80	53.98	50.08
crossed (approx C_2)	3.51	3.57	43.60	48.95

^a See Figure 4 for the structures. ^b c.m. to c.m. distance. ^c BSSE-uncorrected interaction energy.

graphite two-layer structure, Figure 3. The T-shaped dimers of anthracene are significantly less stable than the crossed dimer.⁹ As in the case of the benzene dimer and the naphthalene trimer, there is an excellent agreement between the MP2 and HFD dimer binding energies and geometries. Interestingly, the D_{2d} crossed geometry of the anthracene dimer was also found to be the global minimum in the structure predictions^{24,25} based on the exp-6-1 atom-atom interaction potential²⁶ and the geometry search²⁷ based on the model potential of Claverie.²⁸

Table 5 compares the MP2 and HFD intermolecular potentials for the pyrene dimers. For pyrene, all low-energy dimer conformers have “stacked” structures of very similar energies, Figure 4. The lowest energy conformer is the C_{2h} slip-parallel structure, which can be generated from the D_{2h} sandwich dimer via shear along the long (L) in-plane axis (i.e., the axis parallel to the central C–C bond), Table 5. The next in order are the C_i graphite two-layer structure and the C_{2h} slip-parallel structure that can be obtained from the sandwich dimer by shear along the short (S) in-plane axis, Figure 4. The crossed dimer of approximate C_2 geometry is less stable than the three slip-parallel structures. The differences in binding energies are however so small (especially for the three slip-parallel structures)

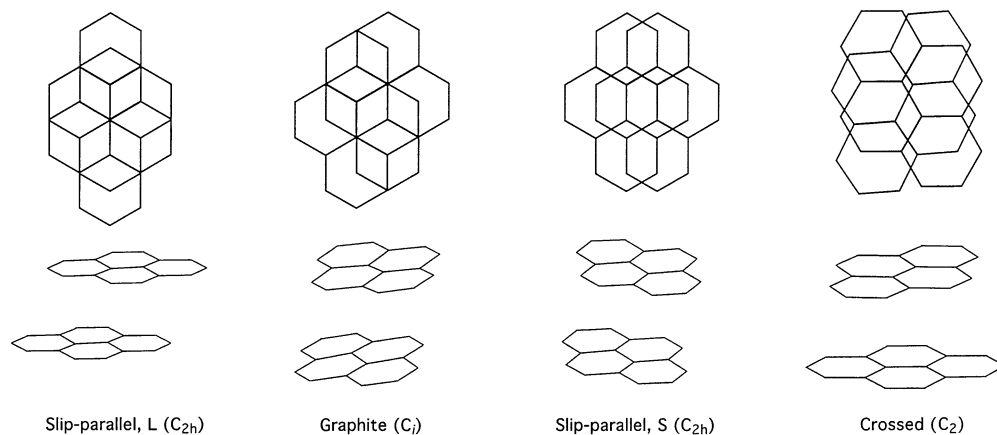


Figure 4. Top and side views of the low-energy MP2/6-31G and HFD/6-31G dimer structures of pyrene.

that it is not possible to predict the global minimum of the pyrene dimer. The small energy difference indicates that the potential energy surface is very shallow with respect to shear. It is interesting that the C_{2h} slip-parallel, *L* structure corresponds to the projection of one pyrene molecule on the plane of its parallel neighbor in the dimeric structure of the pyrene crystal.²⁹ The computed interplanar separation of 3.51 Å (MP2) is in excellent agreement with the interplanar distance of 3.53 Å in the crystal.

D. Comparison of the HFD Model with the Valence-Bond-Based Model Potential. The major shortcoming of the MP2/6-31G and HFD/6-31G methods is that the computed binding energies are significantly greater than the experimental binding energies for the dimers of benzene and naphthalene, and for the trimer of naphthalene. The MP2 calculations with the larger and diffuse basis sets do even more poorly, as illustrated for the naphthalene dimers (Table 2).

Very recently an alternative hybrid method, incorporating valence bond (VB) theory and the intermolecular potential of Claverie,²⁸ has been utilized by Bouvier et al.³⁰ to probe equilibrium geometries and binding energies of small neutral and ionic clusters of aromatic hydrocarbons. Interestingly, this VB-based model potential yields binding energies of the benzene dimer, and the dimer and trimer of naphthalene, which are in good agreement with the experimental values. Unfortunately, the significance of this energy agreement is not clear and even questionable, as the T-shaped minimum energy structures of the naphthalene and anthracene dimers predicted by the method differ from the stacked structures computed by all other methods (MP2, HFD, exp-6-1, and other model potentials). No further comparison of the performance of the HFD and VB-based model potential is warranted in the absence of the experimental geometries for naphthalene and anthracene dimers.

E. Propensity Rules for the Dimer Geometry and Size Dependence of Dimer Binding Energy. Despite the absence of the experimental dimer geometries, some useful proposals concerning the preferred dimer geometry can be made from the calculated HFD/6-31G and MP2/6-31G binding energies, Tables 1–5. Present work, as well as earlier studies,^{4,7,9–12} indicates that the equilibrium geometry of an aromatic dimer is determined by the balance of electrostatic (quadrupole–quadrupole) interaction and dispersion. Different geometries can be adapted depending upon the relative importance of the two interactions. When the contribution of the electrostatic interaction to the dimer binding energy is not small, electrostatic interactions would favor an edge-on structure^{7,14,31,32} as in the T-shaped dimer of benzene. For the polycyclic aromatic hydrocarbons, the dominant contribution of dispersion interaction would favor

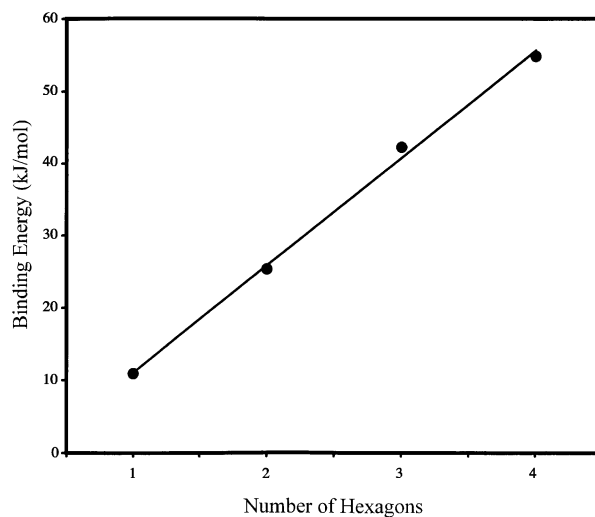


Figure 5. Plot of the MP2/6-31G binding energy of the minimum-energy dimer conformer as a function of the number of hexagons in the monomer.

stacked geometries of deformed sandwich configuration. The deformation, which reduces nonbonded repulsions, could involve shear or rotation of one of the monomers relative to the other. When the monomer is substantially longer than it is wide, as in anthracene, the D_{2d} crossed dimer may be favored over the C_{2h} slipped structure due to the greater attractive dispersion contribution.^{9,11} For a molecule that is almost as wide as it is long, as in pyrene, the parallel-displaced (slip-parallel) structure with maximum π – π overlap would be preferred.

Interestingly, the calculated HFD/6-31G and MP2/6-31G binding energies (Tables 1–5) of low-energy conformers are approximately a linear function of the number of hexagons in the monomer, as shown in Figure 5. This correlation is reasonable because the contribution of the dispersion interaction to the dimer binding energy is expected to increase with the increasing size of the interacting monomers.

4. Conclusions

The most significant result of this study is that the simple HFD/6-31G model predicts intermolecular potentials of the dimers of benzene, naphthalene, anthracene, and pyrene that are nearly identical to those obtained from the MP2/6-31G calculations. This is fortunate since most of the aromatic clusters are too large to be considered even by the relatively modest MP2/6-31G level of theory. Although computationally efficient, the density functional theory (DFT) with the existing exchange-correlation function, have not proven to be reliable for aromatic

clusters.^{11,33,34} A similar situation also exists for the atom–atom (or site–site) potentials.³⁵ In view of the success of the MP2/6-31G calculations in accounting for the experimental geometries of the benzene dimer and naphthalene trimer, the remarkable agreement between the MP2 and HFD intermolecular potentials points to the utility of the HFD/6-31G model for probing equilibrium geometries of aromatic clusters.

Despite their success in reproducing experimental geometries, the HFD/6-31G and MP2/6-31G methods yield binding energies that are significantly greater than the experimental values for the dimers of benzene and naphthalene and the trimer of naphthalene. The reason for these discrepancies is very likely due to the use of a small basis set and incomplete treatment of electron correlation by MP2. A practical solution to this difficulty may be to perform an MP2 single point energy calculation on the optimized HFD/6-31G geometry, using a large basis set and the counterpoise correction. The utility and the practicality of such an approach are presently under investigation in our laboratories.

Acknowledgment. We are grateful to the Office of the Basic Energy Sciences of the Department of Energy for support of this work and to the Ohio Supercomputer Center for generous grants of computer time. We also thank Prof. Seung Keun Kim for a preprint of ref. 10, Dr. Tiffany Walsh for providing the coordinates for the C₂ crossed dimer of naphthalene, and Profs. Janet Del Bene and Richard Friesner for helpful comments.

References and Notes

- (1) Arunan, E.; Gutowsky, H. J. *Chem. Phys.* **1993**, *98*, 4294.
- (2) Benharash, P.; Gleason, M. J.; Felker, P. M. *J. Phys. Chem. A* **1999**, *103*, 1442.
- (3) Dunning, T. H., Jr. *J. Phys. Chem. A* **2000**, *104*, 9062.
- (4) See ref 5 for a recent summary.
- (5) Sinnokrot, M. O.; Valeev, E. F.; Sherrill, C. D. *J. Am. Chem. Soc.* **2002**, *124*, 10887.
- (6) Grover, J. R.; Walters, E. A.; Hiu, E. T. *J. Phys. Chem.* **1989**, *91*, 3233.
- (7) Tsuzuki, S.; Honda, K.; Uchimura, T.; Mikami, M.; Tanabe, K. *J. Am. Chem. Soc.* **2002**, *124*, 104.
- (8) Gonzalez, C.; Lim, E. C. *J. Phys. Chem. A* **1999**, *103*, 1437.
- (9) Gonzalez, C.; Lim, E. C. *J. Phys. Chem. A* **2000**, *104*, 2953.
- (10) Lee, N. K.; Park, S.; Kim, S. K. *J. Chem. Phys.* **2002**, *116*, 7910.
- (11) Walsh, T. R. *Chem. Phys. Lett.* **2002**, *363*, 45.
- (12) Gonzalez, C.; Allison, T. C.; Lim, E. C. *J. Phys. Chem. A* **2001**, *105*, 10583.
- (13) Hepburn, J.; Scoles, G.; Penco, R. *Chem. Phys. Lett.* **1975**, *36*, 451.
- (14) See, for review: Stone, A. J. *The Theory of Intermolecular Forces*; Clarendon: Oxford, U.K., 1996.
- (15) Peng, C.; Ayala, P. Y.; Schlegel, H. B.; Frisch, M. J. *Comput. Chem.* **1996**, *17*, 49.
- (16) Certain commercial materials and equipment are identified in this paper in order to specify procedures completely. In no case does such identification imply recommendation or endorsement by the National Institute of Standards and Technology, nor does it imply that the material or equipment identified is necessarily the best available for the purpose.
- (17) Frisch, M. J.; et al. *GAUSSIAN 98*; Gaussian, Inc.: Pittsburgh, PA, 1998.
- (18) GAMESS: Schmidt, M. W.; et al. *J. Comput. Chem.* **1993**, *14*, 1347.
- (19) Huiszoon, C.; Mulder, F. *Mol. Phys.* **1979**, *38*, 1497.
- (20) Krause, B.; Ernstberger, B.; Neusser, H. J. *Chem. Phys. Lett.* **1991**, *184*, 411.
- (21) Fujiwara, T.; Lim, E. C. *J. Phys. Chem. A* **2003**, *107*, 4381.
- (22) Tsuzuki, S.; Uchimura, T.; Matsumura, K.; Mikami, M.; Tanabe, K. *Chem. Phys. Lett.* **2000**, *319*, 547.
- (23) On the basis of the MM3 vibrational frequencies, we estimate the zero-point energy of about 3 kJ/mol for the naphthalene dimer. For the T-shaped benzene dimer, Sherrill and co-workers⁵ report a value of about 1.5 kJ/mol.
- (24) Xiao, Y.; Williams, D. E. *Chem. Phys. Lett.* **1993**, *215*, 17.
- (25) White, R. P.; Niesse, J. A.; Mayne, H. R. *J. Chem. Phys.* **1998**, *108*, 2208.
- (26) Williams, D. E.; Xiao, Y. *Acta Crystallogr. A* **1991**, *2*, 219.
- (27) Piuze, F.; Dimicoli, I.; Mons, M.; Millié, P.; Brenner, V.; Zhao, Q.; Soep, B.; Tramer, A. *Chem. Phys.* **2002**, *275*, 123.
- (28) Claverie, P. *Intermolecular Interactions: From Diatomics to Biopolymers*; Wiley: New York, 1978.
- (29) Birks, J. B. *Photophysics of Aromatic Molecules*; Wiley-Interscience: London, 1970.
- (30) Bouvier, B.; Brenner, V.; Millié, P.; Soudan, J. M. *J. Phys. Chem. A* **2002**, *106*, 10326.
- (31) Lim, B. T.; Lim, E. C. *J. Chem. Phys.* **1983**, *78*, 5262.
- (32) Jaffe, R. L.; Smith, G. D. *J. Chem. Phys.* **1996**, *105*, 2780.
- (33) Boo, B. H.; Lim, E. C. Unpublished results, 2001.
- (34) Tsuzuki, S.; Lüthi, H. P. *J. Chem. Phys.* **2001**, *114*, 3949.
- (35) Gonzalez, C.; Lim, E. C. *Chem. Phys. Lett.* **2002**, *357*, 161.